A Distributed Radar Architecture above 100 GHz using Lens Arrays for Sensing Applications

A. Nair[#], G. Carluccio[*], W. Syed[*], H. Nandagopal[*], M. Alonso-delPino[#], D. Cavallo[#], K. Doris[*], N. Llombart[#]

[#]Delft University of Technology, The Netherlands
[*]NXP Semiconductors, The Netherlands
{A.Nair, M.AlonsoDelPino, D.Cavallo, N.Llombartjuan}@tudelft.nl,
{giorgio.carluccio, waqas.syed, harish.nandagopal, kostas.doris}@nxp.com

***Abstract* — This paper presents a distributed radar system architecture designed for sensing applications above 100GHz. The proposed radar system leverages high-gain lens arrays to generate extremely narrow beams, enabling high angular resolution. A hybrid beamforming approach is proposed in both the transmitter and receiver arrays, allowing for continuous scanning across a moderate field of view. Additionally, an ideal estimation of radar range is conducted assuming a simplified radar equation for this architecture, showing its potential to detect targets at very long distances.**

***Keywords* — Angular resolution, Beamforming, Distributed RADAR, Lens Array**

I. INTRODUCTION

There is a growing interest in the high millimeter-wave (sub-THz) spectrum, particularly within the D-band for applications in sensing and communications [1-2]. In certain scenarios, ultra-narrow sensing capabilities in the order of 1° is envisioned [3]. Existing millimeter-wave solutions, such as those operating at 77 GHz, utilize MIMO arrays based on microstrip or slotted waveguide antennas [3-4]; however these suffer from limited resolution and significant distribution losses. The gain of these antennas is typically low, penalizing the detection capabilities at high frequencies, where the signal-to-noise ratio (SNR) is constrained due to the lack of available power. Moreover, these MIMO array architectures suffer from the presence of grating lobes, leading to sensing ambiguities that then require complex ambiguity-resolving algorithms, thereby increasing processing time. Besides, classical phased arrays are difficult to scale up in frequency due to the integration and thermal limitations [5]. In [5], some of the authors proposed the use of lens phased arrays to reach antenna architectures in the sub-THz and THz bands with continuous scanning and high gain using a hybrid electro-mechanical approach.

In this contribution, we propose a high-frequency radar architecture that can be potentially used for sensing applications. The architecture is based on lens arrays, where each lens element exhibits high gain (~30dBi) and is excited by an array of planar antenna elements. On the transmitter side, all the elements are fed coherently. In this case both the element pattern and the array factor can be steered electronically enabling continuous scanning over the desired field of view (FoV). By having the array of antenna elements under the lens, we avoid the mechanical scanning of the element pattern as described in [5] and have instead a fully electronic solution. On the receiver side, each element is processed incoherently and the beamforming is realized digitally.

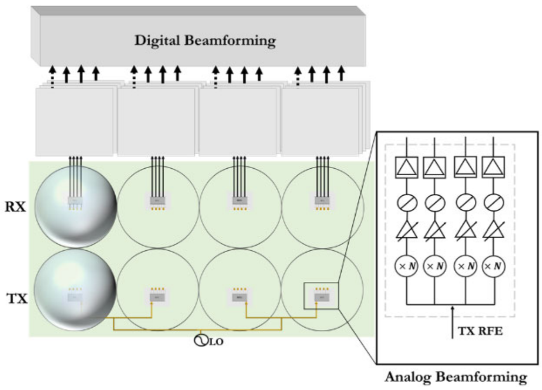

Fig. 1. Distributed Radar Architecture at 140GHz using 1x4 Tx and 1x4 Rx Lens Arrays: below each lens there are antenna elements for electronic steering of the lens array.

II. DISTRIBUTED RADAR SYSTEM ARCHITECTURE

The objective here is to develop a long range radar above 100 GHz with an angular resolution of 1° over a FoV of 18° in the horizontal plane while ideally detecting targets at long range. We assume that there is no scanning in the vertical plane. The architecture is constrained to 16 transmitters and 16 receivers, which are distributed across 8 high-frequency millimeter-wave RF front-end (RFE) chips.

The proposed architecture is as depicted in Fig. 1, where each of the 8 RFEs is integrated below each of the lenses leading to low transition losses between the chip and the planar antennas used to illuminate the lens. This leads to two 1x4 lens phased arrays, one for transmitting and one for receiving. The LO signal is generated on a frequency synthesizer chip and distributed using a PCB to the RFEs. Each of the RFE chips contains 4 Tx or Rx channels that are used to scan the high gain lens element pattern in a desired direction, such that only 2 Tx channels are active per RFE.

The planar antennas used to illuminate the lenses can be slots, dipoles, patches or a combination of those. The spacing between these antennas is optimized to enhance the gain of each individual lens element., i.e., set to $d \sim \lambda_d f_{\#}$ where λ_d is the wavelength in the lens material and $f_{\#}$ is the equivalent focal to diameter ratio of the lens.

The steering of the pattern is performed using a combination of digital and analog beam-scanning architectures where the amplitude and phase of the planar antennas are varied depending on the desired steering direction. Analog beamforming is implemented on the transmitter side. The array factor of the lens array is scanned using in-phase and quadrature (IQ) phase shifters, whereas electronic beamforming is employed to scan the element pattern which is realized by a gain controlled amplifier and phase-shifter connected to each antenna [6]. Complex weights are given to each of the antenna elements placed below a lens in order to perform the electronic beamforming. The methodology used to compute these beamforming weights uses a bi-directional ray-tracing based field matching technique as presented in [7]. Thus allowing continuous scanning in the Tx end for the desired FoV. This configuration in the Tx end enables combining the power from the transmitters over the air via a lens array such that power is collimated into a single directive beam. On the other hand, the receiving array uses a digital beamforming architecture, where the signals received by each of the receiver elements under the lenses are combined after the ADC processing, with associated beamforming weights [7]. Thus resulting in a continuous FoV coverage even at the receiver end. Fig. 2 depicts the two-way (Tx · Rx) pattern showcasing continuous scanning in the FoV.

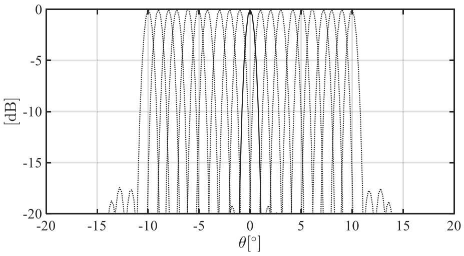

Fig. 2. Two-way pattern depicting continuous scanning of FoV.

III. 1° Angular Resolution and Range

The advantage of utilizing a passive component such as a lens is that its diameter directly determines key parameters, including directivity, half-power beamwidth (HPBW), and the overall profile of the lens antenna. This provides an additional degree of freedom in optimizing the lens array to meet specific design requirements. Additionally, the number of antenna elements positioned beneath each lens defines the FoV coverage of the lens antenna.

In our case, we aim to design the lens antenna elements in order to achieve high gain per element. Therefore each lens element has a diameter of $D_{lens} = 10\lambda_0$, resulting in a high ideal lens directivity of $D^L = 20\log_{10}(\pi D_{lens}/\lambda_0) = 30dBi.$ As described in Section II, there are $N_e = 4$ antenna elements placed under each lens resulting in a FoV $= N_e \frac{\lambda_0}{D_{lens}} \sim \pm 10°$. The associated lens HPBW $= \Delta\theta_{3dB} = \frac{\lambda_0}{D_{lens}} = 5.72°$.

There are $N_l = 4$ lens elements each in the transmitter and receiver side, resulting in a maximum lens array directivity of $D^{LA} = D^L + 10\log_{10}(N_l) = 36dBi$ when coherently combined. The resulting coherent beam has a very narrow HPBW of $\Delta\theta_{3dB}^{LA} = \frac{\lambda_0}{N_l D_{lens}} = 1.4°$ in both the Tx and Rx array. The combined two-way pattern gives the desired ultra-narrow HPBW= $\Delta\theta_{3dB}^{two-way} = \frac{\Delta\theta_{3dB}^{LA}}{\sqrt{2}} = 1°$, as illustrated in Fig. 2.

The planar antenna array to be placed under each lens was designed in package. Furthermore in order to have low scan loss, high gain and low side-lobes, multiple optimization steps were incorporated. The antenna array was placed above the focal plane [8], and the lens was made with different eccentricities in both planes to compensate for the defocusing effect in the orthogonal plane when moving the antenna away from the focus. The final optimised design had a lens spillover efficiency of 80% and showcased a maximum gain of $G_{tx/rx}$ =33.2dBi with a scan loss of $0.8dB$ across the scan range.

Table 1. FMCW Radar Specification

Specifications	Value
Minimum SNR ($\boldsymbol{SNR_{min}}$)	15dB
Average Output Power ($\boldsymbol{P_{out}}$)	7dBm/channel
Noise Figure ($\boldsymbol{F}$)	15dB
Radar Cross-section ($\boldsymbol{\sigma}$)	0-10dBsm
Sampling Frequency ($\boldsymbol{F_s}$)	40MHz

In order to have an estimation of the radar system performance using the lens array, we have presented a set of requirements as stated in Table 1 as a starting point for the system analysis. The classical radar range equation provides the maximum range that can be achieved by a radar having a single transmitting and receiving antenna that uses the entire measuring time for a single beam. If we consider a measuring time of T_{meas}~1ms for a single beam steered to broadside, the radar range equation can be written in terms of the measuring time as shown in equation 1, where $N = 2 \times N_l$ represents the total number of active transmitter channels over the 4 lenses.

$$R_{max}^{LA} = \left[\frac{NP_{out}\, G_{tx}\eta_{tx}G_{rx}\eta_{rx}T_{meas}\lambda_0^2\sigma}{2\,(4\pi)^3 SNR_{min}Fk_bT}\right]^{1/4} \quad (1)$$

For the range analysis we assume $\eta_{tx/rx} =$ 3dB of losses in both the Tx and Rx. We attribute these losses to the connection to the front-end and effect of the radome over the lens array. Fig. 3 shows a comparison of the ideal range that can be achieved by a single Tx/Rx lens to that of the proposed lens antenna array architecture while scanning one beam in 1ms. Here we make the assumption that the transmitter chips can be perfectly synchronized and that there are no further losses.

With respect to the single lens Tx/Rx Radar, the proposed scanning architecture has an improved SNR due to the number of active transmitter elements per chip, over-the-air power combining and the high directivity of the lens array in both Tx and Rx. One can observe that due to the high SNR, this architecture can potentially reach very long distances and hence be considered for long range sensing applications.

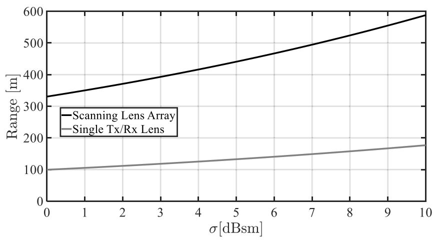

Fig. 3. Ideal range achieved by the scanning lens array architecture compared to a single Tx/Rx lens as a function of radar cross section (σ) given in decibels per square meter.

IV. Prototype and Preliminary Results

The 4 element lens array prototype was fabricated and it is as shown in Fig. 4(a), where under each lens an array of planar antenna designed in package is present. The characterization of the lens antenna array was performed using a measurement test bench setup similar to the one in [9] and it is as depicted in Fig. 4(b). It comprises of a planar near-field scanner based on a CNC machine with a probe station. A VNA with frequency extenders in the WR 6.5 frequency band was used to measure the S-parameters. The one-port probe station uses pico-probes to land onto the antenna elements under the lens. The lens antenna array is placed facing downward, and a 45° metal plate acting as a mirror is used to direct the radiation towards a WR 6.5 open ended waveguide probe connected to a twist which is then connected to WR 6.5 frequency extender mounted on the CNC. Using this setup the radiation pattern and directivity of each of the 16 antenna elements will be characterized.

(a)

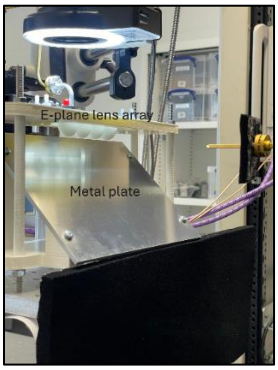

(b)

Fig. 4 (a) Photograph of the fabricated lens antenna array (b) Photograph of the measurement setup

The near-field scanning plane of $10\,\text{cm} \times 10\,\text{cm}$, was placed at a distance of ~10 cm from the tip of the 1st lens. The far-field patterns of each individual element can be calculated using the near-field to far-field transformation. Fig. 5 (a) shows the incoherent far-field pattern of the left most antenna element placed under lens 1 (as shown in Fig. 4(a)), without any time gating. The far-field results are compared to that of the PO simulation from MATLAB and the radiation patterns look comparable to that of the simulation as depicted in Fig. 5 (a). Fig. 5(b) shows the directivity measured over the WR 6.5 frequency range for the same element. The directivity achieved at the central frequency from the measurements is around 27.1dBi and that from the PO code is about 26.3dBi. As a starting point, the radiation pattern achieved from the measurements look promising and the results need to be further investigated for all elements.

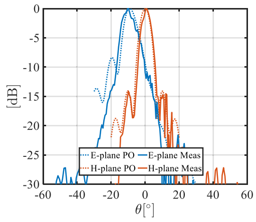

(a)

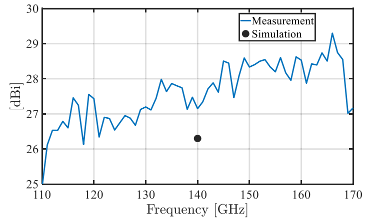

(b)

Fig. 5 (a) Measured far-field radiation pattern in both main planes of the edge antenna element under 1st lens compared to that of PO simulation shown in dotted lines. (b) Measured directivity of the edge lens antenna element over the WR 6.5 frequency range.

V. Conclusion

In this work, we proposed a distributed radar system architecture utilizing lens arrays for long-range sensing applications. The hybrid architecture, incorporating both analog and digital beam scanning, was outlined. Design criteria for the lens array were discussed, focusing on achieving high gain and an angular resolution of 1° while maintaining coverage over a moderate field of view. Additionally, the radar range performance was estimated using a single-beam having a measuring time of ~1ms, assuming ideal conditions. Lastly, preliminary measurements of the fabricated lens array were presented in Section IV. Further measurements for all 16 elements are ongoing to accurately compute the coherent pattern in post-processing. These results will most likely be presented in the conference.

References

[1] M. Köhler, J. Hasch, H. L. Blöcher, and L.-P. Schmidt, “Feasibility of automotive radar at frequencies beyond 00 GHz,” *International Journal of Microwave and Wireless Technologies*, vol. 5, no. 1, pp. 49–54, 2013.

[2] T. S. Rappaport et al., “Wireless Communications and Applications Above 00 GHz: Opportunities and Challenges for 6G and Beyond,” *IEEE Access*, vol. 7, pp. 78729-78757, 2019.

[3] F. G. Jansen et al., "Simultaneous Multi-Mode Automotive Imaging Radar Using Cascaded Transceivers," 2021 18th European Radar Conference (EuRAD), London, United Kingdom, 2022, pp. 441-444.

[4] Q. Ren et al., "Gapwaveguide Automotive Imaging Radar Antenna With Launcher in Package Technology," in IEEE Access, vol. 11, pp. 37483-37493, 2023.

[5] S. Bosma, N. Van Rooijen, M. Alonso-Delpino, M. Spirito and N. Llombart, "First Demonstration of Dynamic High-Gain Beam Steering With a Scanning Lens Phased Array," IEEE Journal of Microwaves, vol. 2, no. 3, pp. 419-428, July 2022.

[6] F. van Vliet and A. de Hek, “Front-end technology for phased-arrays with digital beamforming,” Conf. Microw., Commun.,Antennas Electron. Syst., May 2008.

[7] A. Nair et al., "On the Optimization of Lens Phased Arrays for Continuous Scanning for Sub-THz Sensing Applications," 2024 49th International Conference on Infrared, Millimeter, and Terahertz Waves (IRMMW-THz), Perth, Australia, 2024, pp.1-2.

[8] N. T. Nguyen, M. Casaletti, T. V. La, and R. Sauleau, “Synthesized elliptical lens with optimized extension for focal array fed lens antennas,” Eur. Conf. Antennas Propag., Prague, Czech Republic, 2012, pp. 3295-3298.

[9] N. v. Rooijen et al., "A Core-Shell Lens for Antenna On-Package Integration at D-Band," in IEEE Transactions on Antennas and Propagation, vol. 72, no. 8, pp. 6195-6208, Aug. 2024.